

# Synthesis of BiOI nanobelt and its visible-light photocatalytic activity

Ping-Quan Wang<sup>1</sup>, Yang Bai<sup>1</sup>, Jian-Yi Liu<sup>1</sup>, Zhou Fan<sup>1</sup>, Ya-Qin Hu<sup>2</sup>

<sup>1</sup>State Key Laboratory of Oil and Gas Reservoir Geology and Exploitation, Southwest Petroleum University, Chengdu 610500, People's Republic of China

<sup>2</sup>Civil Affairs Bureau of Karamay District, Xinjiang, Karamay 834000, People's Republic of China

E-mail: baiyanghyq@foxmail.com

Published in Micro & Nano Letters; Received on 3rd October 2012; Accepted on 15th January 2013

BiOI nanobelts were synthesised by a one-pot solvothermal process in the presence of [Bmim]I. As-synthesised BiOI nanobelts showed higher photocatalytic activity in the aqueous RhB photodegradation system than BiOI nanosheets under visible-light irradiation. It could be widely used for the environmental purification of organic pollutants in an aqueous solution.

**1. Introduction:** Semiconductor photocatalysis based on harnessing and converting solar energy into chemical energy has been considered to be a green and promising pathway for solving the energy crisis and eliminating most kinds of contaminants [1, 2]. Recently, Bi(III)-based semiconductors, such as BiVO<sub>4</sub> [3], Bi<sub>2</sub>MO<sub>6</sub> [4], Bi<sub>2</sub>WO<sub>6</sub> [5] and BiPO<sub>4</sub> [6] have been reported to be promising photocatalysts. BiOI is an important V–VI–VII ternary semiconductor compound with a suitable absorption edge at about 670 nm and the estimated bandgap energy of about 1.8 eV. Recently, it also has been established as effectual photocatalysts for the degradation of aqueous dyes under visible-light irradiation [7–10]. BiOI is one of the simplest members of the Sillen family phases, which is expressed either as [Bi<sub>2</sub>O<sub>2</sub>] [L<sub>m</sub>] or [Bi<sub>3</sub>O<sub>4+n</sub>] [L<sub>m</sub>] (*m* = 1–3), where bismuth oxide-based fluorite-like layers, [Bi<sub>2</sub>O<sub>2</sub>] or [Bi<sub>3</sub>O<sub>4+n</sub>], are inter-grown with double chlorine layers [10]. Bi-based oxychlorides attracted considerable attention because of their potential application as novel photocatalysts owing to their unique layered structures and high photocorrosion stability [11, 12].

Many routes have been adopted to synthesise BiOI with various morphologies and have led to successful fabrication. Reverse microemulsions, consisting of heptane, non-ionic surfactants and aqueous salt solutions, were used to synthesise BiOX (*X* = Cl, Br, I) nanoparticles [13]. BiOI nanosheets have been synthesised through phase-transfer-assisted reaction or the precipitation–filtration process [7, 14, 15]. The one-pot solvothermal process was explored to prepare a BiOI three-dimensional (3D) structure by employing ethylene glycol or ethanol–water mixed solvent as the solvent [9, 10]. They exhibited good photoactivity under visible-light irradiation. However, the synthesis of BiOI nanobelts has not been reported until now. In this Letter, we report for the first time a facile route for the synthesis of BiOI nanobelts with dominant {001} facets. The photocatalytic results showed that BiOI nanobelts displayed good photoactivity for RhB photocatalytic degradation (PCD).

## 2. Experimental

**2.1. Synthesis:** Bi(NO<sub>3</sub>)<sub>3</sub>•5H<sub>2</sub>O (AR, 99.0%) was added slowly into an 1-butyl-3-methylimidazolium iodide ([Bmim]I) solution, with the Bi/I molar ratio of 1. The mixture was stirred for 1 h at room temperature in air, and then poured into a 50 ml Teflon-lined stainless autoclave until 80% of the autoclave volume was filled. The autoclave was allowed to be heated at 160°C for 24 h under autogenous pressure, and then air cooled to room temperature. The resulting BiOI nanobelts precipitates were collected and washed with ethanol and deionised water thoroughly and dried at 50°C in air.

As a comparison, BiOCl nanosheets were synthesised by KI replacing [Bmim]I. TiO<sub>2</sub> P25 was purchased from Degussa Co.

**2.2. Characterisation:** Powder X-ray diffraction (XRD) was performed on a Bruker D8-Advance X-ray powder diffractometer with Cu K $\alpha$  radiation ( $\lambda$  = 1.5418 Å). The  $2\theta$  range used in the measurements was from 10 to 70 in steps of 0.028. Field emission scanning electron microscope (FESEM) images were obtained by a JEOL JEM-6700F FESEM operating at an accelerating voltage and applied current of 5 kV and 10 mA, respectively. Transmission electron microscope (TEM) images were taken using a Hitachi model H-800 TEM with an accelerating voltage of 200 kV. The structure and composition of the nanobelts were measured by high-resolution transmission electron microscopy (HRTEM, JEOL-2010F). Absorption measurements were carried out using a Shimadzu UV-2100S spectrophotometer. The Brunauer-Emmett-Teller (BET) surface areas were measured using quantachrome autosorb-1 automated gas sorption systems at 77 K.

**2.3. Photocatalytic reactivity test:** The optical system used for the photocatalytic reaction consisted of a 500 W halogen-tungsten lamp and a 420 nm cutoff filter. The typical PCD process is arranged in this way: 50 ml aqueous suspensions of 10 mg/l RhB was placed in a quartz glass beaker, and then 10 mg photocatalysts were added. Prior to irradiation, the suspensions were sonicated for 10 min and then magnetically stirred in darkness for 30 min to obtain desorption–adsorption equilibrium. A magnetic stirrer was employed for continuous mixing. At certain time intervals, 4 ml suspensions were sampled and centrifuged to remove the particles. The upper clear liquid was analysed by recording the maximum absorption band (553 nm for RhB) and the UV–visible spectra of dyes using a Shimadzu UV-2100S spectrophotometer.

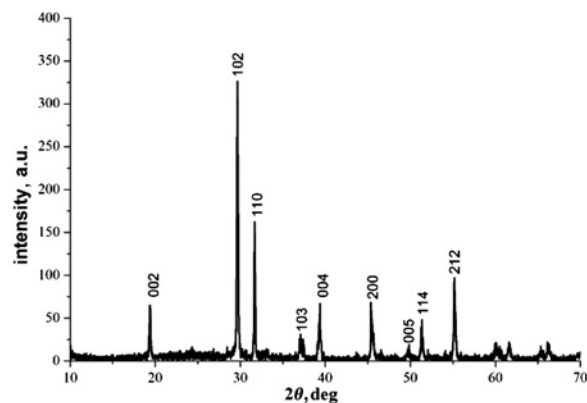
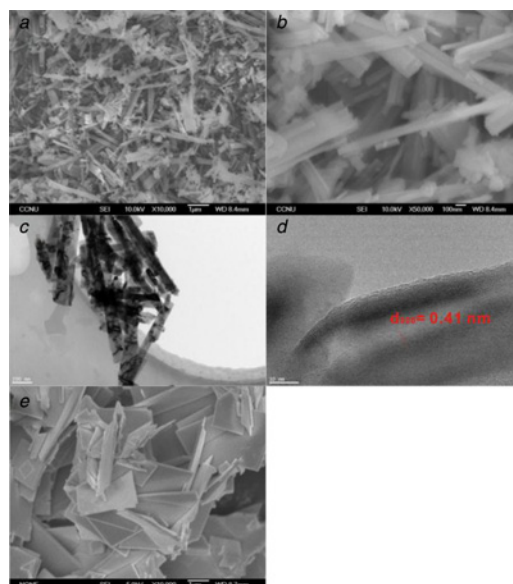


Figure 1 XRD pattern of the BiOI nanobelts

**3. Results and discussion:** Fig. 1 shows the XRD pattern of the BiOI nanobelts with sharp peaks, which indicates the good crystal quality of the BiOI nanobelts. It can be found that there are three peaks (002), (102) and (110) at  $2\theta$  of  $19.36^\circ$ ,  $29.57^\circ$  and  $31.71^\circ$ , respectively. All the diffraction peaks can be indexed to the tetragonal structure of BiOI with a space group of  $P4/nmm$  (JCPDS, 85-0863). The X-ray photoelectron spectroscopy (XPS) measurements provided further information for the evaluation of the purity and surface composition of the BiOI nanobelts. The XPS survey spectrum in Fig. 2a demonstrates no peaks of elements other than C, O, Bi and I in the sample, a proof of the purity of BiOI nanobelts. Fig. 2b shows the high-resolution XPS spectra of Bi 4f. The two strong peaks at the Bi regions of 159.1 and 164.4 eV are, respectively, assigned to Bi4f<sub>7/2</sub> and Bi4f<sub>5/2</sub> of BiOI.

Figs. 3a and b show the FESEM images BiOI nanobelts. It can be seen that most are single-crystal nanobelts (Fig. 3a). The size of BiOI nanobelts is about  $1000 \times 150$  nm (Fig. 3b). Usually, BiOI is in the morphologies of nanoflakes, nanoplates, aggregative spheres or nanometre particles. Here, BiOI displayed single-crystal nanobelts for the first time. To obtain further the morphology and structure information, the TEM and HRTEM analyses of BiOI nanobelts have been applied. The TEM image also shows single-crystal nanobelts with the same size as shown in FESEM images. The HRTEM image of a single BiOI nanobelt crystal (Fig. 3d) shows clearly lattice fringes with a lattice spacing of 0.41 nm, corresponding to that of the {020} facets. Thus, the crystal growth of the nanobelt appears to follow the [020] zone direction [16]. Fig. 3e shows the FESEM images of referenced BiOI sample. It can be seen that the sample was nanosheets.

Fig. 4 shows the UV-vis absorption spectra of BiOI nanobelts. It can be seen that the absorption band ranges from 300 to 600 nm,



**Figure 3** BiOI nanobelts  
a and b FESEM images  
c TEM image  
d HRTEM image  
e FESEM image of BiOI nanosheets

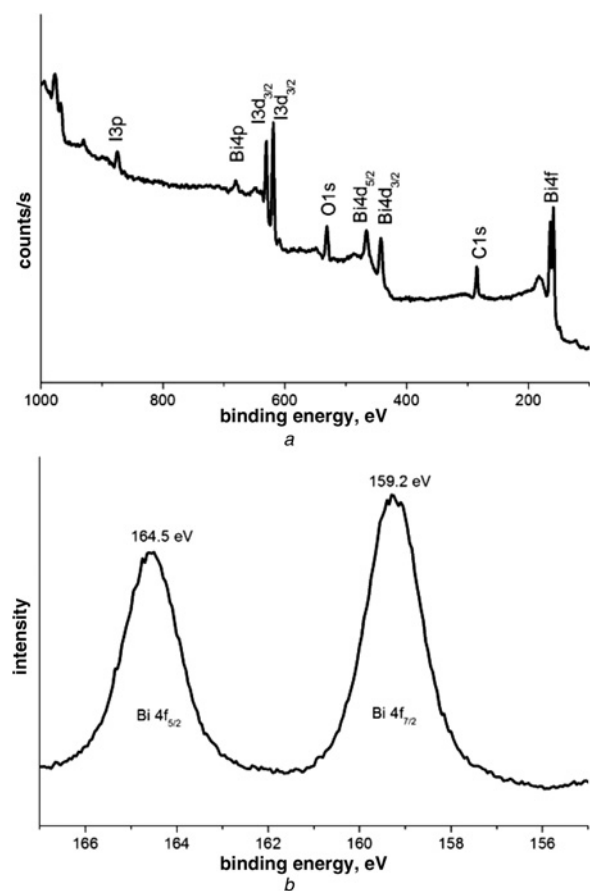


**Figure 2** BiOI nanobelts  
a XPS survey spectrum  
b High-resolution XPS spectra of Bi 4f

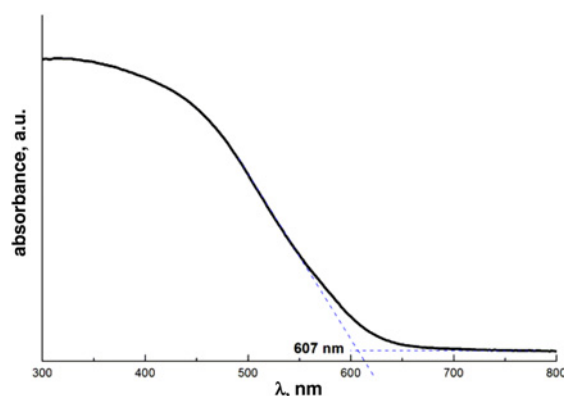


**Figure 4** UV-vis absorption spectra of BiOI nanobelts

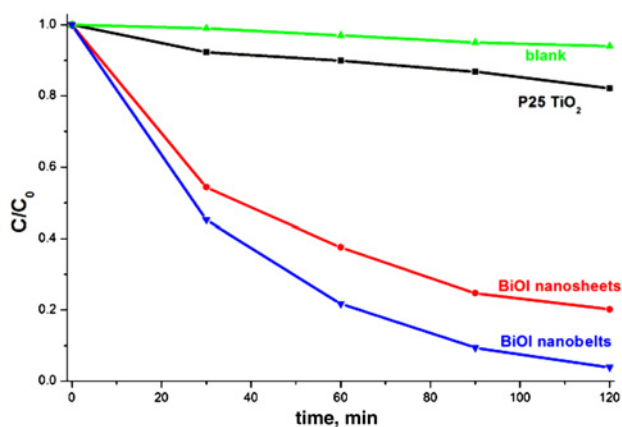


**Figure 5** Photocatalytic activity of BiOI nanobelts under visible-light irradiation

with high absorption. The obvious absorption edge is located at about 607 nm in the visible-light region. The bandgap energy of BiOI nanobelts and irregular BiOI are estimated to be 1.83 eV. This observed bandgap agrees well with the previous reports [17–20]. Red BiOI nanobelts can absorb most of visible light and be excited under sunlight irradiation.

RhB is one kind of organic azo dye that is often used as a model pollutant to study the catalytic performance of photocatalysts [21, 22]. In this study, RhB was chosen as the target pollutant to trace the photocatalytic activity of BiOI nanobelts under visible-light irradiation. The PCD experiments of RhB by BiOI nanobelts and BiOI nanosheets were comparatively performed (Fig. 5). Under visible-light irradiation, the BiOI nanobelts (BET surface area is 11.2 m<sup>2</sup>/g) show much better photocatalytic activity than BiOI nanosheets (BET surface area is 13.4 m<sup>2</sup>/g) and P25 TiO<sub>2</sub>.

**4. Conclusions:** In this reported work, BiOI nanobelts were synthesised by a one-pot solvothermal process in the presence of [Bmim]I. As-synthesised BiOI nanobelts showed higher photocatalytic activity in the aqueous RhB photodegradation system than BiOI nanosheets under visible-light irradiation. It could be widely used for the environmental purification of organic pollutants in an aqueous solution.

**5. Acknowledgments:** This work was supported by the seventh installment of the Graduate Innovation Fund of Southwest Petroleum University (grant no. GIFSB0704).

## 6 References

- [1] Ye L., Zan L., Tian L., Peng T., Zhang J.: 'The {001} facets-dependent high photoactivity of BiOCl nanosheets', *Chem. Commun.*, 2011, **47**, pp. 6951–6953
- [2] Wang P.Q., Bai Y., Liu J.Y., Fan Z., Hu Y.Q.: 'N, C-codoped BiOCl flower-like hierarchical structures', *Micro Nano Lett.*, 2012, **7**, pp. 876–879
- [3] Dunkle S.S., Helmich R.J., Suslick K.S.: 'BiVO<sub>4</sub> as a visible-light photocatalyst prepared by ultrasonic spray pyrolysis', *J. Phys. Chem. C*, 2009, **113**, pp. 11980–11983
- [4] Zhang L., Xu T., Zhao X., Zhu Y.: 'Controllable synthesis of Bi<sub>2</sub>MoO<sub>6</sub> and effect of morphology and variation in local structure on photocatalytic activities', *Appl. Catal. B*, 2010, **98**, pp. 138–146
- [5] Wang C., Zhang H., Li F., Zhu L.: 'Degradation and mineralization of bisphenol A by mesoporous Bi<sub>2</sub>WO<sub>6</sub> under simulated solar light irradiation', *Environ. Sci. Technol.*, 2010, **44**, pp. 6843–6848
- [6] Pan C., Zhu Y.: 'New type of BiPO<sub>4</sub> oxy-acid salt photocatalyst with high photocatalytic activity on degradation of dye', *Environ. Sci. Technol.*, 2010, **44**, pp. 5570–5574
- [7] Chang X., Huang J., Tan Q., *ET AL.*: 'Photocatalytic degradation of PCP-Na over BiOI nanosheets under simulated sunlight irradiation', *Catal. Commun.*, 2009, **10**, pp. 1957–1961
- [8] Lei Y., Wang G., Song S., *ET AL.*: 'Room temperature, template-free synthesis of BiOI hierarchical structures: visible-light photocatalytic and electrochemical hydrogen storage properties', *Dalton Trans.*, 2010, **39**, pp. 3273–3278
- [9] Xiao X., Zhang W.D.: 'Facile synthesis of nanostructured BiOI microspheres with high visible light-induced photocatalytic activity', *J. Mater. Chem.*, 2010, **20**, pp. 5866–5870
- [10] Zhang X., Ai Z., Jia F., Zhang L.: 'Generalized one-pot synthesis, characterization, and photocatalytic activity of hierarchical BiOX (X = Cl, Br, I) nanoplate microspheres', *J. Phys. Chem. C*, 2008, **112**, pp. 747–753
- [11] Ye L., Tian L., Peng T., Zan L.: 'Synthesis of highly symmetrical BiOI single-crystal nanosheets and their {001} facet-dependent photoactivity', *J. Mater. Chem.*, 2011, **21**, pp. 12479–12484
- [12] Hahn N.T., Hoang S., Self J.L., Mullins C.B.: 'Spray pyrolysis deposition and photoelectrochemical properties of n-type BiOI nanoplatelet thin films', *ACS Nano*, 2012, **6**, pp. 7712–7722
- [13] Henle J., Simon P., Frenzel A., Scholz S., Kaskel S.: 'Nanosized BiOX (X = Cl, Br, I) particles synthesized in reverse microemulsions', *Chem. Mater.*, 2007, **19**, pp. 366–373
- [14] Luz A., Feldmann C.: 'Phase-transfer assisted synthesis of BiOI nanoplatelets, quantum-confined color and selective modification of surface conditioning', *Solid State Sci.*, 2011, **13**, pp. 1017–1021
- [15] Li Y., Wang J., Yao H., Dang L., Li Z.: 'Efficient decomposition of organic compounds and reaction mechanism with BiOI photocatalyst under visible light irradiation', *J. Mol. Catal. A, Chem.*, 2011, **334**, pp. 116–122
- [16] Deng H., Wang J., Peng Q., Wang X., Li Y.: 'Controlled hydrothermal synthesis of bismuth oxyhalide nanobelts and nanotubes', *Chem. Eur. J.*, 2005, **11**, pp. 6519–6524
- [17] Liu M., Zhang L., Wang K., Zheng Z.: 'Low temperature synthesis of δ-Bi<sub>2</sub>O<sub>3</sub> solid spheres and their conversion to hierarchical BiOI nests via the Kirkendall effect', *Cryst. Eng. Commun.*, 2011, **13**, pp. 5460–5466
- [18] Zhang X., Zhang L.: 'Electronic and band structure tuning of ternary semiconductor photocatalysts by self doping: the case of BiOI', *J. Phys. Chem. C*, 2010, **114**, pp. 18198–18206
- [19] Wang Y., Deng K., Zhang L.: 'Visible light photocatalysis of BiOI and its photocatalytic activity enhancement by in situ ionic liquid modification', *J. Phys. Chem. C*, 2011, **115**, pp. 14300–14308
- [20] Li Y., Wang J., Liu B., Dang L., Yao H., Li Z.: 'BiOI-sensitized TiO<sub>2</sub> in phenol degradation: a novel efficient semiconductor sensitizer', *Chem. Phys. Lett.*, 2011, **508**, pp. 102–106
- [21] Ye L., Liu J., Gong C., Tian L., Peng T., Zan L.: 'Two different roles of metallic Ag on Ag/AgX/BiOX (X = Cl, Br) visible light photocatalysts: surface plasmon resonance and Z-scheme bridge', *ACS Catal.*, 2012, **2**, pp. 1677–1683
- [22] Ye L., Deng K., Xu F., Tian L., Peng T., Zan L.: 'Increasing visible-light absorption for photocatalysis with black BiOCl', *Phys. Chem. Chem. Phys.*, 2012, **14**, pp. 82–85